

# Imaging and Focusing of an Atomic Beam with a Large Period Standing Light Wave

T. Sleator<sup>\*</sup>, T. Pfau, V. Balykin, and J. Mlynek

Fakultät für Physik, Universität Konstanz, W-7750 Konstanz, Fed. Rep. Germany

Received 20 December 1991/Accepted 6 February 1992

**Abstract.** A novel atomic lens scheme is reported. A cylindrical lens potential was created by a large period ( $\simeq 45\ \mu\text{m}$ ) standing light wave perpendicular to a beam of metastable He atoms. The lens aperture ( $25\ \mu\text{m}$ ) was centered in one antinode of the standing wave; the laser frequency was nearly resonant with the atomic transition  $2^3S_1 - 2^3P_2$  ( $\lambda = 1.083\ \mu\text{m}$ ) and the interaction time was significantly shorter than the spontaneous lifetime (100 ns) of the excited state. The thickness of the lens was given by the laser beam waist ( $40\ \mu\text{m}$ ) in the direction of the atomic beam. Preliminary results are presented, where an atomic beam is focused down to a spot size of  $4\ \mu\text{m}$ . Also, a microfabricated grating with a period of  $8\ \mu\text{m}$  was imaged. We discuss the principle limitations of the spatial resolution of the lens given by spherical and chromatic aberrations as well as by diffraction. The fact that this lens is very thin offers new perspectives for deep focusing into the nm range.

**PACS:** 32.80.-t, 42.50.Vk, 07.77.+P

The focusing of atomic beams is a field of intense activity. One motivation for this activity is the use of a neutral atomic beam as a sensitive and high resolution microprobe. Neutral atoms as probing particles, because of their relatively high mass, have very low energy (for a given de Broglie wavelength), and therefore should cause minimal damage to the sample. The fact, that atoms have a complex internal structure opens new possibilities to study surface properties.

Lenses in general are based on either refraction or diffraction. An ideal refraction lens for neutral atoms must be based on a conservative interaction. Except for magnetic focusing [1], the main interest of research has concentrated on the interaction of atoms with light. Previous experiments have been performed using stimulated light forces in a copropagating Gaussian laser beam [2] as well as using spontaneous light forces [3]. Both methods suffer from aberrations due to either the large thickness of the lens or spontaneous emission.

Recently our group succeeded in imaging and focusing of an atomic beam using a microfabricated Fresnel zone plate [4]. This lens overcomes the problems mentioned above but suffers from significant losses in intensity due to absorption losses as well as diffraction losses into orders other than the first order. Moreover, the focal length, the diameter and the

resolution of this lens are restricted by the limits of present microfabrication techniques.

In this paper we report on the demonstration of a novel (cylindrical) lens scheme which overcomes these problems. Our lens is used to focus a supersonic beam of metastable He atoms using the optical dipole force on the  $2^3S_1 - 2^3P_2$  transition ( $\lambda = 1.083\ \mu\text{m}$ ). The setup is based on a large period standing wave ( $\simeq 45\ \mu\text{m}$ ) produced by bouncing a laser beam off a glass surface under very small angle of incidence (10 mrad). The thickness of the interaction region is less than  $80\ \mu\text{m}$  resulting in an interaction time (40 ns) much shorter than the natural lifetime ( $\tau = 100\ \text{ns}$ ) of the atomic excited state  $2^3P_2$ . Therefore, spontaneous emission is essentially avoided even in the case of very powerful resonant light. The focal length is only restricted by the laser power; in our experiment this focal length was about 30 cm. The spherical aberration is smaller than that in a copropagating laser beam, using e.g., a  $\text{TEM}_{01}^*$  mode [5–7]. As the laser beam is perpendicular to the atomic beam, the construction and the alignment of the setup are easy to perform.

## 1 Basic Properties of a Lens Based on a Standing Wave

We briefly describe the theory of the dipole force in a standing wave. A two-level atom interacts with a light field given by  $\mathbf{E}(\mathbf{r}, t) = \text{Re}\{\hat{\epsilon}E_0(\mathbf{r})\exp(i\omega t)\}$ , where  $E_0(\mathbf{r})$  is the spa-

<sup>\*</sup> Present address: New York University, Department of Physics, NY 10003, USA

tially varying electric field amplitude and  $\hat{\varepsilon}$  is the polarization vector. We model the field produced in our experiment by

$$E_0(\mathbf{r}) = E_{0,max} \cos(k_x x) e^{ik_y y} e^{-z^2/w_0^2}. \quad (1)$$

Equation (1) describes a standing wave with period  $2\pi/k_x$  in the  $x$ -direction, a traveling wave in the  $y$ -direction, and a gaussian beam profile with beam waist  $w_0$  in the  $z$ -direction, which is the direction of the atomic beam. We assume that the atom enters the light field in the ground state  $|g\rangle$  with momentum  $p$ , and that the interaction time of the atom with the field is much shorter than the lifetime  $\tau$  of the excited state  $|e\rangle$ . The velocity  $v$  of the atoms along the beam axis ( $z$ -axis) is considered to be sufficiently large so that the spatial dependence of  $E_0(\mathbf{r})$  along  $\hat{\mathbf{z}}$  can be replaced with the explicit time dependence  $t = z/v$ . Therefore, we replace the factor  $\exp(-z^2/w_0^2)$  in (1) with  $\exp(-t^2/t_i^2)$ , where  $t_i = w_0/v$ . For simplicity we ignore the dependence of the optical field on  $y$ . With the above assumptions, the behavior of the atom in a light field can be described by a one dimensional Schrödinger equation with an interaction Hamiltonian  $H_I = -\mathbf{d} \times \mathbf{E}(\mathbf{r}, t)$ , with atomic dipole moment operator  $\mathbf{d}$ . Diagonalizing the interaction Hamiltonian yields two eigenvectors for the internal state [8]. The corresponding eigenvalues are

$$U_{\pm}(x, t) = \pm(\hbar/2)\sqrt{\Delta^2 + \omega_1^2(x, t)}. \quad (2)$$

Here,  $\omega_1(x, t)$  denotes the spatially dependent Rabi frequency  $\omega_1(x, t) = \langle e|\mathbf{d} \cdot \hat{\varepsilon}|g\rangle E_0(x, t)/\hbar$ .  $\Delta$  is the frequency detuning from resonance. In order to avoid nonadiabatic processes, the laser frequency has to be detuned from resonance by more than a critical value  $\Delta_c$ ; under our experimental conditions, this detuning is  $\Delta_c/2\pi \simeq 30$  MHz (for further discussion see [9, 10]). In this case the internal state of the atom always (adiabatically) follows one of the eigenvectors during the passage through the interaction region.

For an atomic lens centered at an antinode of the standing wave the laser frequency has to be detuned below resonance. In this case all atoms are *strong field seekers* and the potential  $U_-(x, t)$  in (2) represents a cylindrical lens potential. With the assumption  $\Delta \ll \omega_1$ , which is valid in our case, the transverse momentum transfer  $\Delta p$  on the atomic center of mass is given by

$$\Delta p(x) = - \int_{-\infty}^{\infty} \nabla U(x, t) dt = \sqrt{\frac{\pi}{8}} \frac{t_i}{\tau} \hbar k_x \sqrt{\frac{I}{I_S}} |\sin k_x x|. \quad (3)$$

Here,  $I/I_S$  is the ratio of laser intensity and the saturation intensity. For simplicity we assumed a transition with a Clebsch-Gordan coefficient equal to 1. Using the simple geometric relationship  $\Delta p/p = x/2f$  and expanding  $\sin k_x x$  about  $x = 0$  leads to a first order expression for the focal length:

$$f = \sqrt{\frac{8}{\pi}} \frac{\tau}{t_i} \sqrt{\frac{I_S}{I}} \frac{p}{\hbar k_x^2}. \quad (4)$$

The higher order expressions give rise to spherical aberration. A measure for the influence of an aberration is the mean square deviation of the wavefronts from spherical waves af-

ter the passage through the lens. If this deviation is less than  $\lambda/4$  then the limit on the resolution of the lens is given by diffraction. In order to satisfy this so called Rayleigh-criterion for the spherical aberration, the following inequality has to be fulfilled:

$$\frac{1}{48^2} \frac{2\pi}{\lambda_{dB}} k_x^2 \frac{d^4}{f} < \frac{\pi}{2}, \quad (5)$$

where  $d$  is the diameter of the lens, given by the width of the aperture in front of the standing wave.  $\lambda_{dB}$  denotes the de Broglie wavelength, which in our experiments is typically  $0.56 \text{ \AA}$ .

Note that in (4) the following proportionality holds:  $f \propto p/t_i \propto v^2$ . Therefore, fluctuations in the atomic velocity  $v$  lead to chromatic aberrations. The Rayleigh-criterion applied to these chromatic aberrations imposes an upper limit on the relative width of the velocity distribution  $\Delta v/v$  with  $\Delta v$  denoting the full width at half maximum of the atomic velocity distribution

$$\frac{\Delta v}{v} < \sqrt{5} \lambda_{dB} \frac{f}{d^2}. \quad (6)$$

We point out that both conditions (5, 6) are independent of the diameter  $d$  of the lens if we assume that  $k_x d$  and all other parameters in (4) are constant. This means that the lens quality will not be deteriorated if one scales down (or up) a lens (fulfilling the above conditions) by using smaller standing wave periods.

Another important limitation of the resolution of a lens is given by diffraction from the aperture. The minimum spot size cannot be smaller than the width of the central diffraction peak from the lens aperture, which in our case is a slit. The minimum spot size  $\Delta x$  is under our experimental conditions (i.e.,  $f \gg d$  and magnification equal to 1) given by:

$$\Delta x = 2\lambda_{dB} \frac{f}{d}. \quad (7)$$

Since the interaction time is supposed to be much shorter than the excited state lifetime, effects due to spontaneous emission are negligible and diffusive aberration is of no importance.

The limitations by aberrations and diffraction depend on the  $F$ -number  $\equiv f/d$  (see (5-7)). Aberrations can be avoided by using large  $F$ -numbers, whereas the limitation by diffraction is less severe with the use of small  $F$ -numbers.

## 2 Experimental Setup

The experiments were carried out with an atomic beam machine [11] designed for the use with metastable rare gas atoms. A supersonic expansion nozzle at room temperature produced a beam of He atoms, which were then excited into a metastable state by copropagation electrons at an energy of about 31 eV. Both singlet ( $2^1S_0$ ) and triplet ( $2^3S_1$ ) metastable states were produced. The corresponding ratio was measured independently in a deflection experiment to be 40% singlets to 60% triplets. The result was a beam of metastable helium atoms with an average velocity  $v \simeq 1760$  m/s and velocity ratio  $\Delta v/v = 0.05$  with

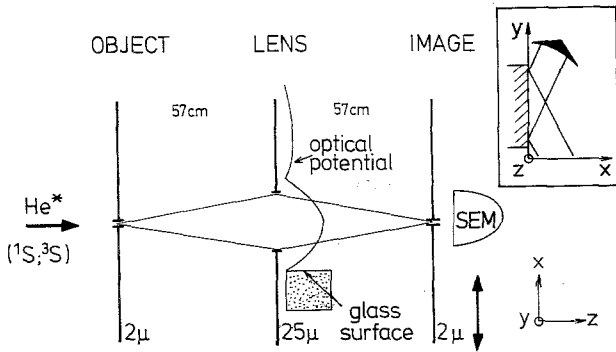


Fig. 1. Schematic diagram of the experimental setup as viewed from above. The optical potential of the standing light wave is indicated. Inset: View along the atomic beam axis of the optical standing wave

$\Delta v$  being the velocity spread. The corresponding de Broglie wavelength is  $\lambda_{dB} = 0.56 \text{ \AA}$ . The beam intensity was about  $10^{13} \text{ He}^*/(\text{sec sr})$ .

In a first experiment, a slit of  $2 \mu\text{m}$  width was used as an object (see Fig. 1). The aperture defining the diameter of the lens was  $25 \mu\text{m}$  wide and placed  $15 \text{ mm}$  upstream from the standing wave. The lateral ( $x$ ) position of the  $25 \mu\text{m}$  slit could be adjusted by a piezo translation stage with high precision allowing us to set the position of the atomic beam within the standing wave. The transverse intensity distribution was measured by mechanically scanning a detector with a  $2 \mu\text{m}$  aperture slit, both attached to a high precision screw, which was turned by a stepper motor. In our experiments the experimental parameters were adjusted such that the focal length was about  $28.5 \text{ cm}$ . The distances object-to-lens and lens-to-detector plane were both  $57 \text{ cm}$ , which corresponds to twice the focal length in the case of a one-to-one image. The slits were aligned parallel to one another by using the diffraction patterns produced by each of the slits when passing the light from a He-Ne laser. The detector, a secondary electron multiplier (SEM), is sensitive to both metastable states but not to ground state atoms.

The triplet  $\text{He}^*$  atoms interact with light at  $1.083 \mu\text{m}$  through the  $2^3S_1$  to  $2^3P_2$  transition. This light was produced by a Ti-sapphire ring laser (Coherent 899-21) pumped with  $27 \text{ W}$  from a  $\text{Ar}^+$  laser. The laser was stabilized on the  $2^3S_1$  to  $2^3P_2$  transition using saturation spectroscopy in a dc helium discharge. A magnetic field with a few percent modulation was applied to the discharge in order to create a dispersion-like error signal, which was fed back to the laser. By varying the dc current through the magnet we were able to control the detuning of the laser frequency from the atomic resonance. The laser output first passed through an intensity stabilizer and was then brought into the beam machine via a single mode optical fiber. The position of the incoupling fiber end was held to maximum output intensity by a feedback loop; in this way the fluctuations in laser power at the experiment were less than 5%. After leaving the fiber, the light was focused by two cylindrical lenses and reflected with grazing incidence off of a glass surface, producing a standing wave with a large period (see inset to Fig. 1). The minimum beam radius in  $z$ -direction was measured to be  $w_0 = 39 \mu\text{m}$ . The beam waist in the  $x$ -direction was  $142 \mu\text{m}$ . The surface was aligned parallel to both the direction of the  $25 \mu\text{m}$  slit (again by laser diffraction techniques) and the

atomic beam axis. Since the angle of the nodal planes of the standing wave to the slit structures is determined entirely by the glass surface, these nodal planes were also parallel to the slits. The precision of this alignment is a prerequisite for high spatial resolution. With an atomic velocity of  $v \approx 1760 \text{ m/s}$ , the interaction time between atoms and light is roughly  $2w_0/v = 44 \text{ ns}$ , significantly less than the  $2^3P$  state natural lifetime of  $100 \text{ ns}$ . For our experiment we had a choice of three nearly degenerate excited states ( $2^3P_{0,1,2}$ ). The results shown in this paper are for the  $J = 1$  triplet metastable state to the  $J = 2$  excited state. No optical pumping was performed, so that each of the magnetic sublevels was equally populated. This fact gives rise to an additional complication because these sublevels have a different coupling strength to the light field, whose values depend on the polarization of the light. In our experiments the light was linearly polarized and therefore the coupling strength of the magnetic sublevels differed only by 15%. This variation in coupling is an additional source of aberration.

### 3 Experimental Results and Discussion

In Fig. 2 we show the intensity profile without light (open circles) representing the geometrical image of the  $25 \mu\text{m}$  wide aperture in front of the standing wave, which was irradiated through the  $2 \mu\text{m}$  wide object structure. In the same graph we show the atomic intensity distribution with the light switched on (full circles). The laser power was about  $3 \text{ mW}$ , corresponding to a Rabi - frequency of about 650 times the inverse lifetime of the excited state  $\Gamma$ , and the laser frequency was red detuned from resonance by  $\Delta/2\pi = 30 \text{ MHz}$ . Due to residual nonadiabatic behavior of the internal states [10] only 85% of the triplets are focussed while 15% are defocussed. The focussed peak does not sit in the center of the shadow of the aperture because the aperture was not centered in the lens potential.

Figure 3 shows the atomic intensity profile for three different values of laser power  $P$ . Here we corrected the signal by taking into account the ratio of the helium triplet and singlet state intensities. The background due to singlets was first calculated and subtracted from the measured intensity distribution. The resulting signal curves were then normal-

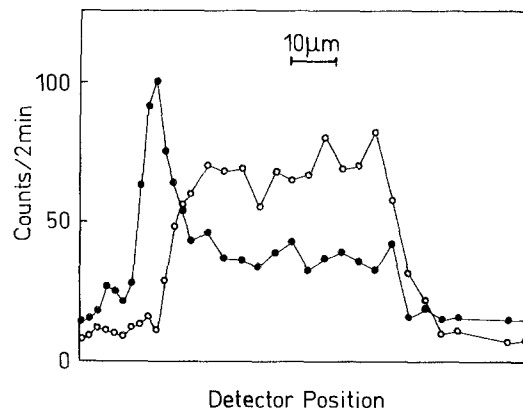


Fig. 2. Intensity in the detector plane using a  $2 \mu\text{m}$  slit as an object ( $\circ$  light off;  $\bullet$  light on); Laser power  $P = 3 \text{ mW}$ , detuning  $\Delta/2\pi = 30 \text{ MHz}$

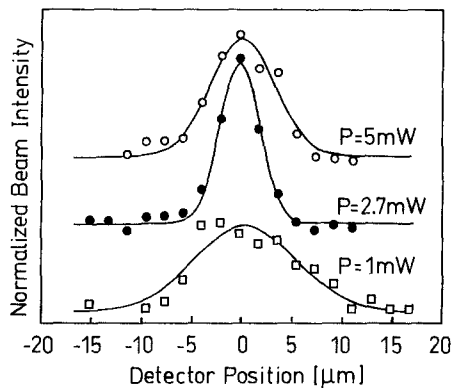


Fig. 3. Corrected atomic intensity in the detector plane using different values of laser power. For further details see text

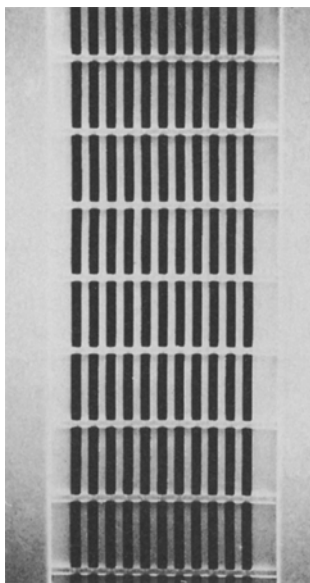


Fig. 4. Scanning electron microscope picture of the grating with period  $8\ \mu\text{m}$ , which was used in the imaging experiment. The horizontal lines show an additional support grid

ized and a Gaussian function was fit to the data, in order to compare the widths. By varying the laser power from  $0.5\ \text{mW}$  to  $5\ \text{mW}$  we varied the focal length of the lens and found a minimum peak width of  $6\ \mu\text{m}$  for a laser power of  $P = 3\ \text{mW}$ . To compute the atomic spot size, we deconvoluted the measured peak with the detector slit ( $2\ \mu\text{m}$ ), which in the case of rectangular intensity distributions leads to a spot size of  $4\ \mu\text{m}$  in the atomic intensity profile. Our measured spot size of  $6\ \mu\text{m}$  has to be compared to the best focussing results published so far, which gave focal spot sizes of  $28\ \mu\text{m}$  using dipole forces [2] and  $18\ \mu\text{m}$  using a Fresnel zone plate [4].

In a second experiment the lens was irradiated by the slits of a grating. The period of this grating was  $8\ \mu\text{m}$  and each slit was  $4\ \mu\text{m}$  wide (see Fig. 4). In Fig. 5 we show the atomic intensity profile in the detector plane. From this preliminary measurement one can clearly identify at least eight peaks at a distance of  $8\ \mu\text{m}$  on a relatively high background due to the singlets. Moreover, this measurement was already at

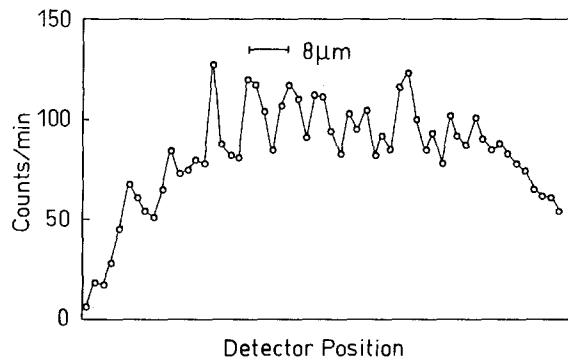


Fig. 5. Intensity in the detector plane showing the one-to-one image of a grating with a period of  $8\ \mu\text{m}$  on a background due to singlets

the limits of the spatial resolution of the detector slit and the lens itself. The result represents the one-to-one image of an one-dimensional object with the resolution in the  $\mu\text{m}$  range. To the best of our knowledge, Fig. 4 also represents the first demonstration of imaging a microstructure using dipole forces.

Let us now discuss our experimental results on the basis of the more general results of the first section. In both focussing experiments the focal length of the lens was  $28.5\ \text{cm}$ . Spherical aberration causes mean square deviations from spherically shaped waves of about  $(\lambda/16)^2$ . The deviation due to chromatic aberration is about  $(\lambda/4)^2$ . In other words, the Rayleigh-criterion for both aberrations is fulfilled under our ideal experimental conditions, however, with the aperture not centered in the lens chromatic aberration will gain significance. The  $F$ -number was  $\sim 11000$  which explains why the aberrations play a minor role. Thus the resolution was limited by diffraction: the minimum spot size that can be achieved with our present lens using a point source as an object is  $\approx 1.5\ \mu\text{m}$ . This value is in good agreement with the measured image size ( $4\ \mu\text{m}$ ) of the  $2\ \mu\text{m}$  wide object.

At the moment the resolution of our setup is also affected by long term thermal drifts in the beam machine as well as by the resolution of our scanning unit for the detector slit. Both problems prevent us from resolving structures in the submicrometer range. For further experiments we plan to overcome these difficulties by stabilizing the beam machine with the feedback from an optical interferometer and by replacing the scanning detector unit by a piezo translation stage.

With the currently available laser power of  $10\ \text{mW}$  and with the use of slower atoms with  $v = 900\ \text{m/s}$ , we could reach focal lengths of about  $5\ \text{cm}$  with the present lens diameter of  $25\ \mu\text{m}$ . In this case the resolution is determined mainly by the chromatic aberration and should be below  $1\ \mu\text{m}$ .

To determine the smallest spot size that we could achieve with our current equipment, we estimated the characteristic parameters of this thin lens for small lens diameters, e.g., in a usual standing wave, where the period is  $\lambda/2$ . Note that for a fixed value of  $k_x d$  and a given laser power, the focal length is proportional to  $d^2/\sqrt{w_0}$  (see (4)), where  $w_0$  represents the thickness of the lens. Therefore, decreasing the thickness of the present lens to a few micrometers would produce a lens with larger focal length that is still diffraction limited

(see (5,6)). In addition, decreasing the lens diameter to about 400 nm ( $\sim \lambda/2$ ) yields a diffraction limited lens with a focal length of about 50  $\mu\text{m}$ . Note that this lens is still thin compared to the focal length. For an atomic velocity of 900 m/s and a laser power of 10 mW the expected spot sizes are in the range of 10 nm. This small spot size can be compared to calculations of McClelland and Scheinfein [6] or Gallatin and Gould [7] done for the thick atomic lens that is based on an off-resonance  $\text{TEM}_{01}$  laser mode copropagating with the atomic beam. Under optimum conditions the authors expect two dimensional spotsizes of comparable size.

#### 4 Conclusion

In conclusion, we have presented preliminary results on a novel atomic lens scheme which overcomes some of the problems arising in previously investigated schemes. The measured spot size of 4  $\mu\text{m}$  is essentially limited by diffraction; chromatic, spherical and diffusive aberrations play a minor role. Moreover, we demonstrated the first imaging of a microstructure by a lens based on the dipole force. Such a thin lens could be used for demagnification or magnification of structures, e.g., in an atom microscope as well as in lithographic techniques. Our scheme could be generalized to two dimensions by combining two standing waves perpendicular to each other.

*Acknowledgements.* We are grateful to G. Jauch for his outstanding work on the construction of the standing wave setup and to A. Schnetz for his help in the final stage of the experiments. Moreover, we thank A. Faulstich, O. Carnal, and M. Sigel for useful discussions. T.S. acknowledges support from the Alexander von Humboldt Foundation. This work was supported by the Deutsche Forschungsgemeinschaft.

#### References

1. H. Friedburg, W. Paul: *Naturwiss.* **38**, 159 (1951); H. Friedburg: *Z. f. Physik* **130**, 493 (1951)
2. J.E. Bjorkholm, R.R. Freeman, A. Ashkin, D.B. Pearson: *Phys. Rev. Lett.* **41**, 1361 (1978); J.E. Bjorkholm, R.R. Freeman, A. Ashkin, D.B. Pearson: *Opt. Lett.* **5**, 111 (1980)
3. V.I. Balykin, V.S. Letokhov, A.I. Sidorow: *J. Mod. Opt.* **35**, 17 (1988)
4. O. Carnal, M. Sigel, R. Sleator, H. Takuma, J. Mlynek: *Phys. Rev. Lett.* **67**, 3231 (1991); M. Sigel: Diploma Thesis, University of Konstanz (1991), unpublished
5. V.I. Balykin, V.S. Letokhov: *Opt. Comm.* **64**, 151 (1987)
6. J.J. McClelland, M.R. Scheinfein: *J. Opt. Soc. Am. B* **8**, 1974 (1991)
7. G.M. Gallatin, P.L. Gould: *J. Opt. Soc. Am. B* **8**, 502 (1991)
8. see e.g., J. Dalibard, C. Cohen-Tannoudji: *J. Opt. Soc. Am. B* **2**, 1707 (1985)
9. A.P. Kasantsev: *Sov. Phys. Usp.* **21**, 58 (1978)
10. T. Sleator, T. Pfau, V. Balykin, O. Carnal, J. Mlynek: Experimental Demonstration of the Optical Stern-Gerlach Effect, submitted to *Phys. Rev. Lett.*; T. Pfau: Diploma Thesis, University of Konstanz (1992) unpublished
11. O. Carnal, A. Faulstich, J. Mlynek: *Appl. Phys. B* **53**, 88 (1991); O. Carnal: Ph.D. Thesis, ETH Zürich No. 9617 (1992), unpublished